European Current Research on Fluid Inclusions (ECROFI-XXI)
Montanuniversität Leoben, Austria, 9–11 August, 2011. Abstracts, p. 188

The effect of post-entrapment crystallization on the H_2O and CO_2 concentrations of rhyolitic (silica-rich) melt inclusions, and implications for magma degassing paths

Steele-MacInnis, Matthew, Esposito, Rosario and Bodnar, Robert J.

Department of Geosciences, Virginia Tech, 4044 Derring Hall, Blacksburg VA 24061 USA

Concentrations of H_2O and CO_2 in silicate melt inclusions (MI) are often interpreted to represent magmatic "degassing paths," in which depressurization of the magma during ascent leads to vapour saturation and release of CO_2 and H_2O from the melt (*e.g.*, Lowenstern, 1994). This interpretation requires that melt inclusions are trapped under conditions of vapour saturation at various locations (depths) along the ascent path. If the trapped melt is saturated in volatiles, then the melt must exsolve a volatile phase if any post-entrapment crystallization occurs. As a result, the pressure inside the MI may differ from the confining pressure during post-entrapment cooling, and the PT path of the MI may be calculated knowing the solubility of H_2O and CO_2 in the melt as a function of T and P, as well as the PVT properties of the H_2O-CO_2 volatile phase, the partial molar volumes of H_2O and CO_2 in the melt, and the molar volumes of the melt phase and the crystallizing solid phase. Using PVTX data for the systems $NaAlSi_3O_8$-H_2O (Burnham and Davis, 1974) and $NaAlSi_3O_8$-H_2O-CO_2 (Holloway and Blank, 1994), we investigate the effect of small fractions of post-entrapment crystallization on the dissolved volatile content in an albitic melt inclusion entrapped under conditions of volatile saturation. The model is constrained to be a closed, isochoric system. As small amounts of albite crystallize on the inclusion walls, the melt becomes supersaturated in volatiles, and so nucleation and growth of an H_2O, CO_2 or H_2O-CO_2 vapour bubble occur and the pressure inside the MI is estimated from the difference between the molar volume of the volatile phase and the partial molar volume of the volatile in the melt using the EOS for H_2O-CO_2 (Holloway, 1977; Flowers, 1979).

Significantly different styles of PT and volatile evolution occur in MI that are saturated with an H_2O-rich fluid versus a CO_2-rich fluid at the time of entrapment (Fig. 1). The differences are due to 1) the higher density of free CO_2 compared to H_2O at magmatic PT conditions, and the larger partial molar volume of CO_2 compared to H_2O in the melt phase; 2) the lower solubility of CO_2 compared to H_2O in the melt phase; and 3) the negative dP/dT slope of the H_2O-saturated solidus compared to the positive dP/dT slope of the CO_2-saturated solidus (Fig. 1). As a result, for CO_2-rich compositions the pressure in the MI and the dissolved CO_2 content of the melt phase both

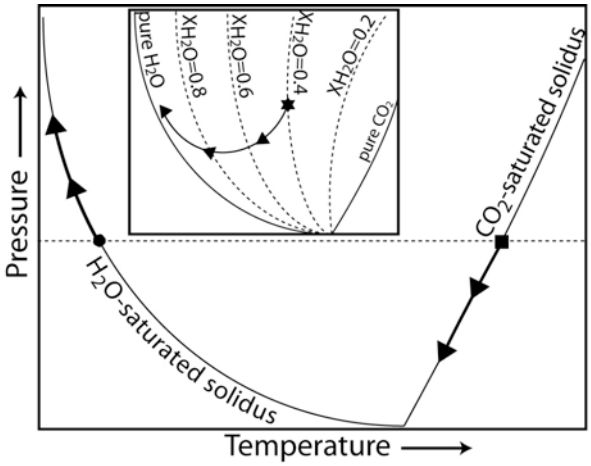

Fig. 1. Schematic PT trajectories followed by vapour-saturated MI during post-entrapment crystallization. Melt-volatile phase relations are shown by the H_2O- and CO_2-saturated solidus curves. The solid circle shows the PT point of entrapment of an H_2O-saturated melt inclusion at the same pressure (dashed line) as a CO_2-saturated melt inclusion shown by the solid square. Thick curves with arrows show the PT paths followed by both MI during PEC. The inset shows the PT path of a mixed H_2O-CO_2 saturated MI trapped at the PT point shown by the star, with isopleths of H_2O in the vapour phase shown as dashed lines).

decrease during post-entrapment crystallization. For H_2O-rich melts, the pressure and the dissolved H_2O concentration in the melt phase both increase during post-entrapment crystallization. Because the solubility of CO_2 in the melt is much lower than that of H_2O, MI with mixed H_2O-CO_2 initial volatile compositions undergo a transition from pressure decrease to pressure increase during post-entrapment crystallization, and the H_2O concentration in the exsolved volatile phase increases as crystallization proceeds (Fig. 1).

The evolution of H_2O and CO_2 contents in the melt (glass) phase during post-entrapment crystallization of volatile saturated MI in some cases reasonably reproduces the observed distribution of H_2O-CO_2 contents of natural MI (e.g., Fig 2). In particular, the dissolved CO_2 content in MI is highly sensitive to small fractions of post-entrapment crystallization, such that nearly all the dissolved CO_2 in the melt phase can be lost during crystallization of a few percent of the melt.

Model results show that dissolved volatile contents in the melt vary in a systematic manner during low degrees of post-entrapment crystallization. More importantly, the H_2O and CO_2 contents of the melt (glass) in the inclusion define trends similar to those produced during open-system degassing. Furthermore, the model predicts that the dissolved CO_2 in the melt phase may be almost completely lost to the vapour phase during post-entrapment crystallization, even though the vapour bubble occupies less than one volume percent of the melt inclusion (Fig. 2). Thus, melt inclusions that all trap a vapour-saturated melt with the same volatile concentrations, but experience varying degrees of post-entrapment crystallization on the walls, will define an H_2O-CO_2 concentration trend resembling an open-system degassing path.

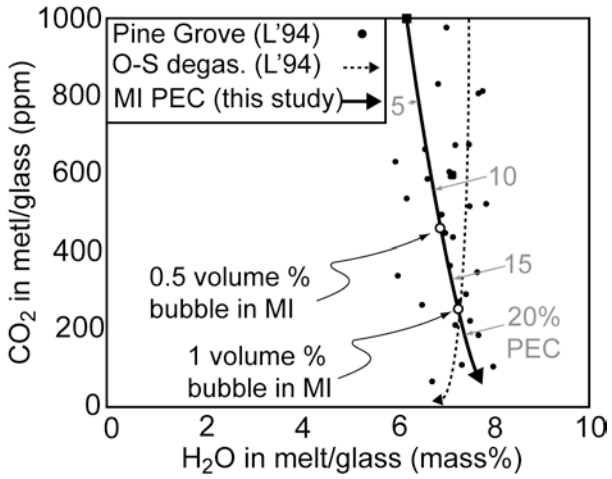

Fig. 2. H_2O-CO_2 contents of MI from Pine Grove, southwest Utah (solid circles, L'94 = Lowenstern, 1994; dashed curve, O-S degas. = open-system degassing; PEC = post-entrapment crystallization). Dashed curve represents open system degassing of a rhyolitic magma at 675 °C from Lowenstern (1994), and solid curve represents post-entrapment crystallization of a rhyolitic MI entrapped at 877 °C, calculated in the present study. Both trends start at 4 kbars. For post-entrapment crystallization, open circles show where the vapour bubble occupies 0.5 and 1 percent of the MI volume. Tic marks and numbers (5, 10, 15, 20%) on the PEC path show the proportion of the melt that has crystallized during PEC.

REFERENCES

Burnham C.W., Davis N.F. (1974) *Am. J. Sci.* 274: 902-940.

Flowers G.C. (1979) *Contrib. Mineral. Petr.* 69: 315-318

Holloway, J.R. (1977) in D.G. Fraser (ed.) *Thermodynamics in Geology*. 161-181

Holloway J.R., Blank J.G. (1994) *Rev. Mineral.* 30: 187-225

Lowenstern J.B. (1994) *Geology* 89: 893-896.